Available online at http://scik.org
Eng. Math. Lett. 2018, 2018:3
https://doi.org/10.28919/eml/3944
ISSN: 2049-9337

ESTIMATION OF POSSIBLE DAMAGES FOR FRAGMENTATION BASE FRAGMENTS ON HUMAN AT DIFFERENT POSTURES

KASHIF ZAHIR*, SALMA SHERBAZ, ADNAN MAQSOOD

Research Center for Modeling and Simulation, National University of Sciences and Technology, Islamabad 54000, Pakistan

Abstract. High Energy Materials causes a sudden release of high pressure, which cause fragmentation of encapsulating shells. For protection from these fragments which contain certain mass, area and velocity we need to know how much these fragments covered distances from fragmentation point. Damage due to fragments is associated with certain probability while covering some distances. Fragments in 2D and 3D fragmentations have certain probability of damage depending on mass, total fragments and distance from fragmentation point.

Keywords: damage study; fragment trajectory; explosive effects; effected area.

2010 AMS Subject Classification: 03F30.

1. Introduction

Estimation of safety distance during development of ordnance storage sites is a trivial problem for military installations. The safety distance is estimated with the perspective that any

*Corresponding author

E-mail address: kashifzaheeer@gmail.com

accidental explosion should result in minimum loss of life and property. The explosions typically generate high pressure shock waves that travel through the air along with the debris resulting from fragmentation of the explosive shells. Analytical approximation of fragment size and shape during any explosion is the most important step in safety distance calculation. Rosin and Rammlers [1] are the first who provided an empirical description of fragmentation in which fragment size distributions were predicted by sorting fragments in different size ranges. Later on, Weibull [2] suggested similar distribution by analyzing the fracture of material under repetitive stresses. Simultaneously Gates-Gaudin-Schuhmann distribution [3] evaluated the particle size distribution data in communication processes [4, 5, 6, 7]. NF Mott [8, 9] formulated the fragments mass distribution for the data obtained through explosive rupture of cylindrical bombs. At the same time Lineau [10] modelled fragmentation as the random geometric fracture of an infinite one-dimensional body. In his study, a line of infinite length was considered that was about to break down into several fragments. Voronoi-Dirichlets formulation has extensively applied in analysis of giraffe skin and honeycomb, cosmology [11], climate modelling [12], crystallography [13] and fracture mechanics [14]. In two dimensional analysis it started with a random placement of points on the plate and space discretized by the construction of orthogonal bisecting lines. Kiang [15] showed that symmetrical high order gamma function provide fragment size distributions for Voronoi-Dirichlets formulation. Grady and Kipps in a series of analysis [16, 17, 18] find that Mott and Linfoot distribution which used for exploding steel cylinders did not necessarily gave the best fitting distribution in multiple dimensions. Despite differences with the Mott and Linfoot distribution, Grady and Kipps keep the same linear exponential function for both area and volume. Some author like Wilbur K. Brown [19] considered fragmentation as a sequential process. Fragment mass distribution in sequential fragmentation is usually described by a cumulative distribution function rather than a probability density function which is more sensitive to the scatter of fragment mass data. The cumulative numbers of fragments is defined as $N_T(m) = N_T(> m)$ with the mass greater than m and alternatively, the cumulative fragment mass $M_T(m) = M_T(> m)$ is the total mass of all fragments with individual mass greater than m. For fragments of considerable size the Mott Formula give a fair estimate. However the Mott did not provide an upper limit of fragment size. It was Stromsoe[20] who

provide formulation to account maximum fragment size. The problem of characterizing the distribution of particles from fragmentation experiments always approached empirically. Most recently Predrag Elek and Slobodan [21, 22] redefine well known Mott Distribution as a Generalized Mott Distribution for different dimension. In section 3 we discuss the detailed procedure which exploits the mass values obtained in fragmentation, the initial velocity of each fragments and drag used in our fragments trajectory model. Probability of damage based on Mott Fragmentation Distribution is also discussed in this section. In section 4 we draw results based on Mott 2D and 3D Fragmentation Distribution. In section 5 we concluded our analysis.

2. Method

The fragmentation and fragment formation due to the explosion of a shell is a random process and cannot be defined exactly. Therefore probabilistic approaches are generally used for the assessment of fragment and their hazard. The fragments produced from the detonation of a single weapon can be characterized by fragment numbers with respect to fragment mass, and their initial velocity. The velocity is estimate by using the Gurney Formula for each type of high energy material being used in the shell. Each Fragment has certain mass, velocity, area, drag coefficient at the point of fragmentation. Fragments displacement is calculated through the fragment trajectory model [23]

Fragment Trajectory Model

Fragment trajectories under the action of drag and gravity forces are calculated using

$$m\frac{d^2x}{dt^2} = -\frac{1}{2}A_\rho C_D V\frac{dx}{dt} \tag{1}$$

$$m\frac{d^2y}{dt^2} = -\frac{1}{2}A_\rho C_D V\frac{dy}{dt} - mg \tag{2}$$

$$m\frac{d^2z}{dt^2} = -\frac{1}{2}A_\rho C_D V\frac{dz}{dt} \tag{3}$$

Where m is the mass of fragment, A is the presented area of the fragment, C_D is the drag coefficient is the density of air,g is the acceleration due to gravity and V is the instantaneous

velocity. Velocity is resolved into three components for our three dimensional trajectory model. To resolved velocity is considered for (0^0 - 360^0) and (0^0 - 180^0). MATLAB solver ode45, based on Runge-Kutta method is used to solve the above system of nonlinear differential equations

$$V = \sqrt{\left(\frac{dx}{dt}\right)^2 + \left(\frac{dy}{dt}\right)^2 + \left(\frac{dz}{dt}\right)^2} \tag{4}$$

Fragment Mass

Predrag Elek and Slobodan [21, 22] redefined well known Mott Distribution as a Generalized Mott Distribution for different dimension

$$N(m) = e^{-\left(\frac{m}{\mu}\right)^{\frac{1}{\lambda}}} \tag{5}$$

$$\mu^{1/2} = B(t^{\frac{5}{6}} d^{\frac{1}{3}})\left(1 + \frac{t}{d}\right) \tag{6}$$

where $N(m)$ is the number of fragments with respect to mass greater than m, is mean fragment mass, t is the thickness of casing, d is the diameter of casing and B is the constant and is specific for a given explosive-metal pair. Distribution Mean used in the Mott fragmentation model is 2μ and 6μ for 2D and 3D respectively

$$N_T = \frac{M}{\mu} \tag{7}$$

$$m_{2D}^{MAX} = -\mu\left(log\left(\frac{2\mu.N(m)}{M}\right)\right)^2 \tag{8}$$

$$m_{3D}^{MAX} = -\mu\left(log\left(\frac{6\mu.N(m)}{M}\right)\right)^3 \tag{9}$$

Where N_T is the total number of fragments for the Mass of a cylinder used,M is the mass of cylinder used for storing the High Energy Explosive Materials, m_{2D}^{MAX},m_{3D}^{MAX} are maximum

masses for our analysis based on total number of fragments in 2D and 3D fragmentations. We suppose that minimum mass value is around zero. We vary the mass values from minimum to maximum to avoid negative values for $N(m)$

Fragment Projected Area

We assume that the fragments generated by a high energy material are geometrically similar, then mass m and presented area A are related by the shape factor k

$$M = kA^{\frac{3}{2}} \tag{10}$$

For our analysis

$$A = (M/k)^{\frac{2}{3}} \tag{11}$$

The values of shape factor or ballistic density k are calculated empirically from ballistic tests for a given weapon. In case of forged steel projectiles the average value of $2.60 g/cm^3$ is recommended [24]

Drag

Fragments moving through the air will experience drag, a force due to pressure and shear stress on the surface of an object in the direction of flow. This force is a combination of normal and tangential forces on the body. Fragments velocities lies in the supersonic regime due to high energy materials, therefore a drag coefficient [23] of 1.21 is used for different types of irregular shapes in our analysis

Probability of Damage

Depending on Generalized Mott distribution, Areal Density q of fragments on a surface away from the fragmentation point [25] is

$$q = \frac{Q_0}{4R^2} e^{\sqrt{2\frac{m}{m_0}}} \tag{12}$$

Where Q_0 is the Total Number of Fragments, m_0 is the Mean Fragment Mass, R is Radius, m is the fragment mass

Where A_T is the area human at different postures[26], the table 1 given below give different area values for different postures

Posture Positions and their Area Values

Index	Posiure	Area
1	Standing	$0.58m^2$
2	Assaulted	$0.37m^2$
3	Supine	$0.10m^2$

$$p = 1 - e^{-qA_T} \tag{13}$$

Where p is probability of Damage

Ballistic Coefficients and Gurney Constants values are obtained from [27]. These values are show in Table below

Ballistic Coefficients and Gurney Constants

Explosive Type	$B\left(\frac{kg^{1/2}}{m^{7/6}}\right)$	$G\left(\frac{m}{s}\right)$
Comp B	2.7026	2,774
RDX	2.5809	2,926
TNT	3.3113	2,499
Tetryl	3.7983	2,438

3. Results and Discussion

Fragment Mass Values in 2D and 3D Fragmentations

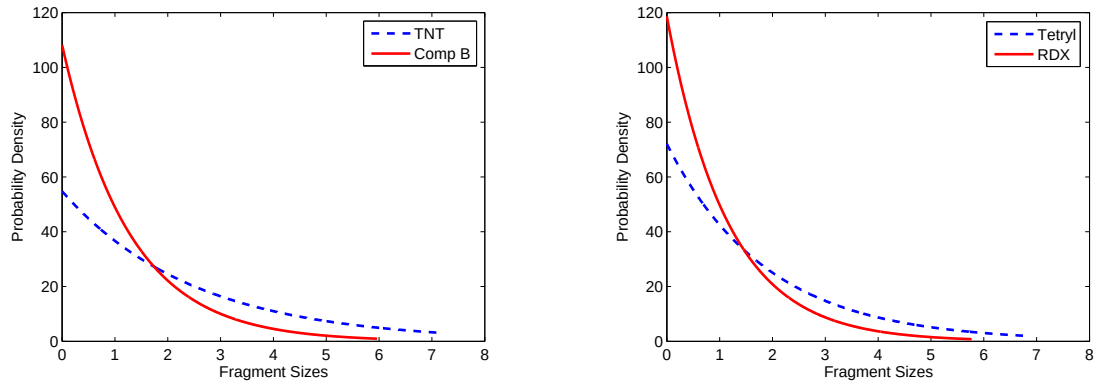

(A) (B)

FIGURE 1. Fragmentation Pattern for 2D Mott Distribution

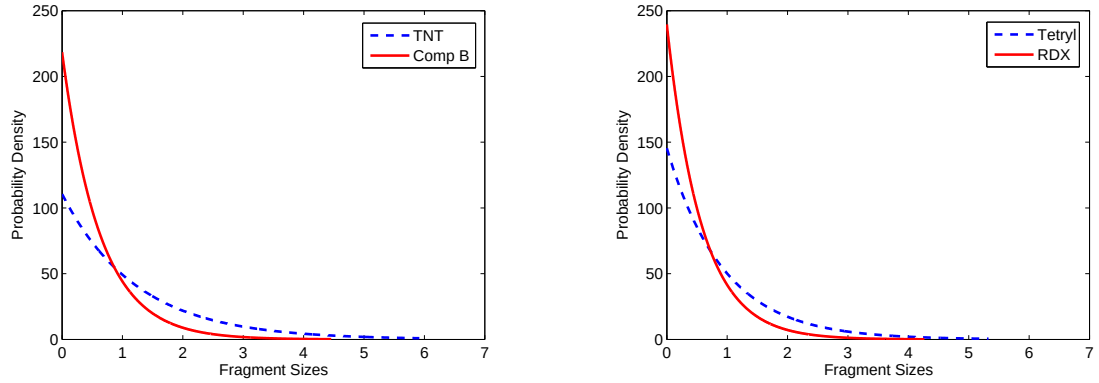

(A) (B)

FIGURE 2. Fragmentation Pattern for 2D Mott Distribution

Fragmentation of projectiles or warheads produces the fragments of different masses and geometries. These explosion based fragments are expected to cause severe damage to the human body at a certain distance. The important parameters required to estimate the risks of human injury from fragments of cylindrical shells include, number and mass distribution of fragments, geometrical shape, the initial velocity and their spatial distribution.

- 2D fragmentation of cylindrical shell produces the fragments of uniform thickness
- 3D fragmentation implies fractures through all three dimensions of a fragmenting body and produces the fragments with size $t* < t$ (shell thickness)

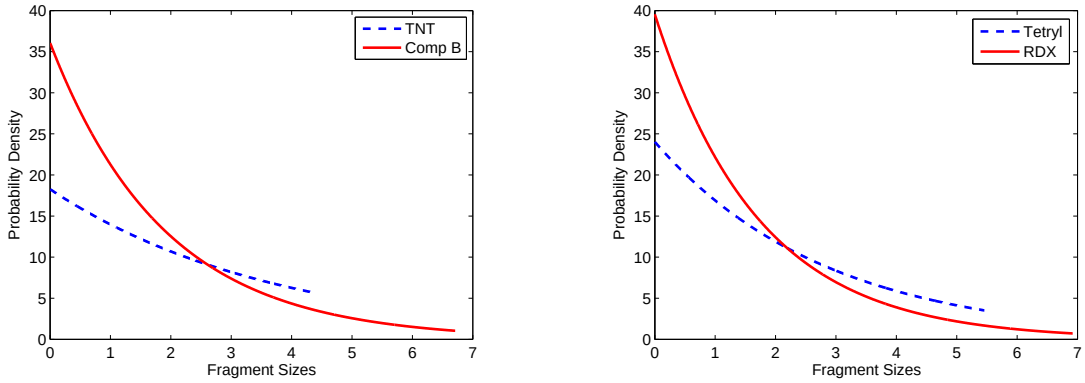

(A) (B)

FIGURE 3. Fragmentation Pattern for 3D Mott Distribution

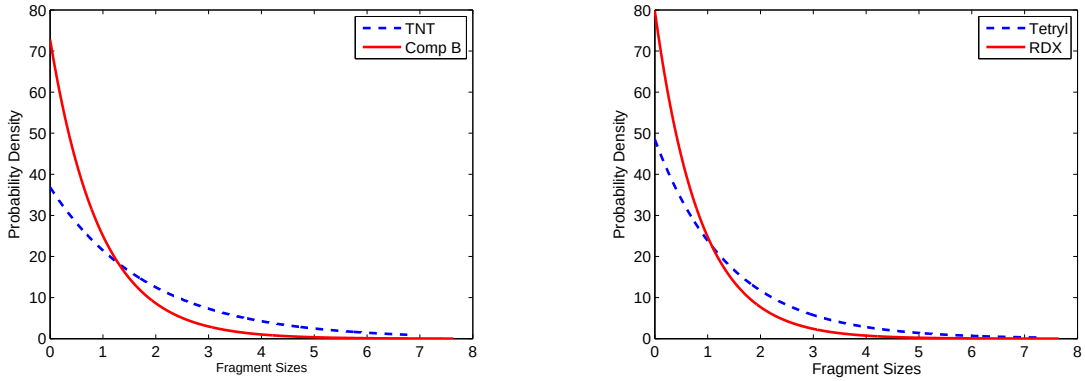

(A) (B)

FIGURE 4. Fragmentation Pattern for 3D Mott Distribution

The Mott formulae are used for estimation of fragmentation number and mass distribution. The parameter used in our analysis is shown in the table below

Shell Parameters

No	Parameters	Values
1	Length	1.54m
2	Mass	136.5kg
3	Diameter	0.2740m
4	Thicknes	0.2m,0.15m
5	Explosive	81.7kg

Figure 1 (a, b) show fragmentation pattern based on 2D Mott Distribution for shell with a thickness of $0.2m$. The total number of fragments generated, are estimated to be 108, 55, 119 and 72 for Comp B, TNT, RDX and Tetryl explosive materials respectively. It can be observed that in all four cases light fragments are produced in large numbers. The largest mass in case of Comp B and TNT are $5.9622kg$ and $7.1396kg$ respectively. As these are largest mass values, all fragments have mass smaller than $5.9622kg$ for Comp B and $7.1396kg$ for TNT. Largest mass in case of RDX and Tetryl for a thickness of $0.2m$, are $5.7682kg$ and $6.7415kg$ respectively. As these are largest mass values, all fragments have mass smaller than $5.7682kg$ for RDX and $6.7415kg$ for Tetryl.

Figure 2 (a, b) show fragmentation pattern based on 2-D Mott Distribution for shell with a thickness of 0.15m. The total number of fragments generated, are estimated to be 218, 111, 240, and 146 for Comp B, TNT, RDX and Tetryl explosive materials respectively. The largest mass in case of Comp B and TNT for second value of thickness are $4.4572kg$ and $5.9168kg$ respectively. As these are largest mass values for thickness of $0.15m$, all fragments have mass smaller than $4.4572kg$ for Comp B and $5.9168kg$ for TNT. Largest mass in case of RDX and Tetryl for thickness of $0.15m$, are $4.2656kg$ and $5.3292kg$ respectively. These being largest mass values, all fragments have mass smaller than $4.2656kg$ and $5.3292kg$ for RDX and Tetryl.

Figure 3 (a, b) shows the fragmentation pattern based on 3D Mott Distribution by considering four different types of explosives (Comp B, TNT, RDX and Tetryl) with a shell thickness of $0.2m$. The total number of fragments generated are estimated to be 36, 18, 40 and 24 for Comp B, TNT, RDX and Tetryl explosive respectively. The masses of the largest fragment in case of Comp B and TNT are $6.7085kg$ and $4.3624kg$ respectively. As these are largest mass values, all fragments have mass smaller than $6.7085kg$ for Comp B and $4.3624kg$ in case of TNT explosive. On the other hand largest mass in case of RDX and Tetryl for shell thickness of $0.2m$, are $6.9196kg$ and $5.4573kg$ respectively.

Figure 4 (a, b) shows the fragment mass distribution in 3D fragmentation of the cylindrical shell with Comp B, TNT, RDX and Tetryl type explosive for thickness of $0.15m$. The total number of fragments generated, are estimated to be 73, 37, 80 and 49 for Comp B, TNT, RDX and Tetryl explosive materials respectively. The largest mass in case of Comp B and TNT for second value

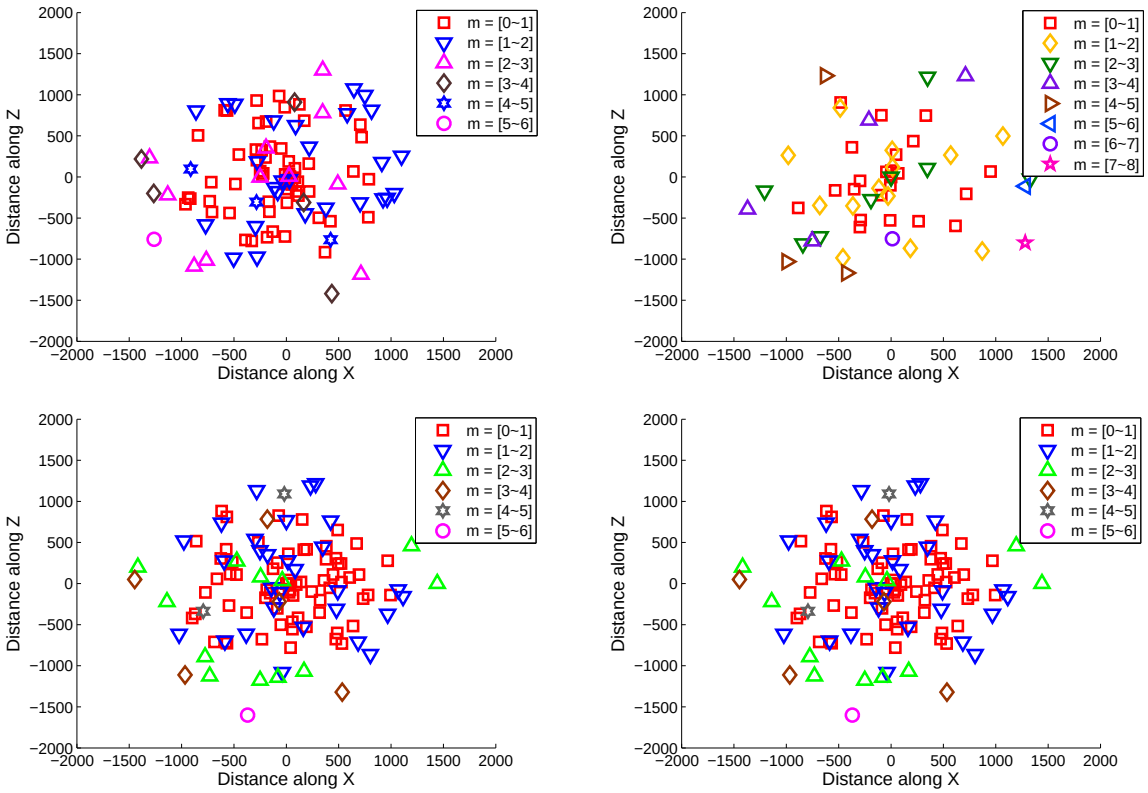

FIGURE 5. Dispersion Map with 2D Fragmentation for Shell with thickness of $0.2m$

of thickness are $7.6328kg$ and $6.7608kg$ respectively. Similarly, the largest mass in the case of RDX and Tetryl, are $7.6454kg$ and $7.2880kg$ respectively.

Distance Travel By Fragments and Dispersion Maps

To calculate risks related to fragmentation (lethality range) of high energy materials, trajectories of different fragments are calculated. The influence of air drag and gravity force has been taken into account. The initial values of velocity [28] components in X, Y, Z directions are calculated for different values of initial throwing angles and . During the trajectory calculation, all fragments are assumed to have same initial fragment velocity. The ground distribution of fragments is determined by terminating the trajectory at the ground level (when y = 0). Fragments of small mass disperse around the fragmentation point while fragments of larger mass disperse at for distance from the fragmentation point. We used four different types of Explosive materials Comp B. RDX, TNT and Tetryl. Materials such as TNT and RDX are secondary

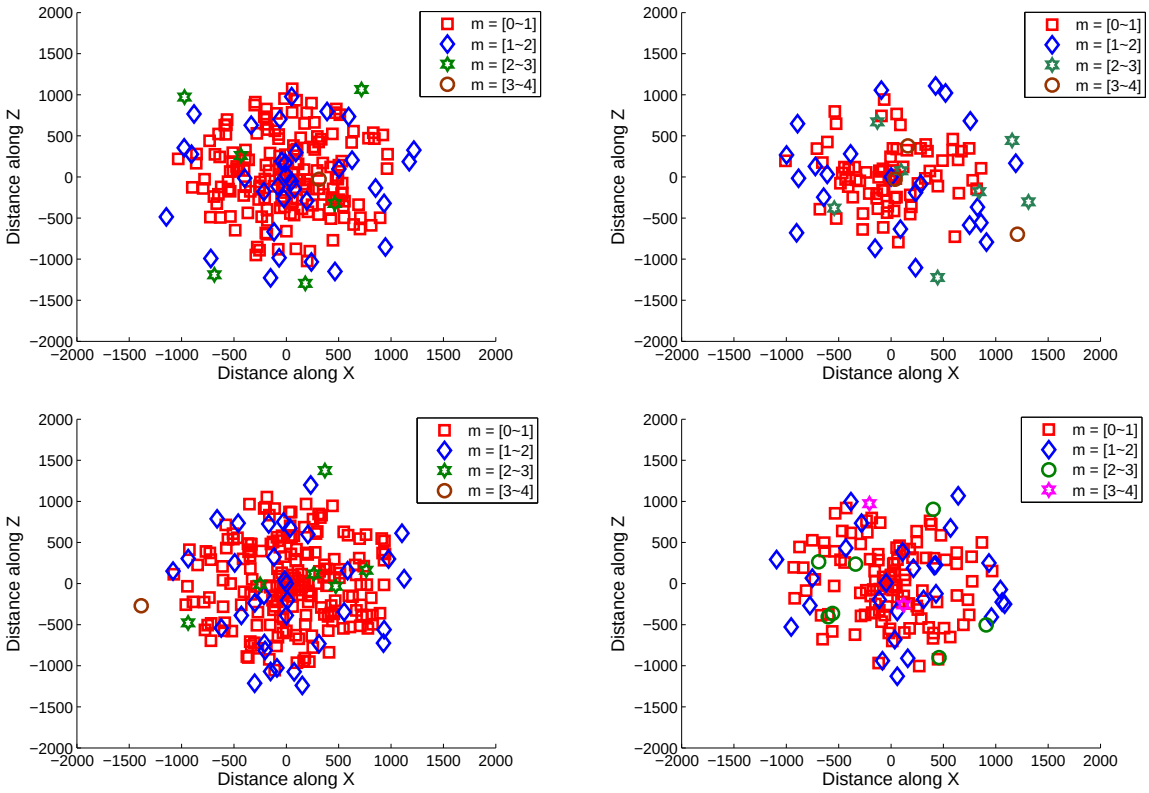

FIGURE 6. Dispersion Map with 2D Fragmentation for Shell with thickness of 0.15m

explosive [29].

Figures 5 and 6 show the dispersion of different fragments in case of 2D Fragmentation for each explosive types (Comp B, RDX, TNT and Tetryl) with shell thickness values (0.2m and 0.15m). The fragment mass and initial throwing angles are randomly sampled. The maximum distance travel by fragments is around 1500m in case of 0.2m shell thickness while for thickness of 0.15m shell thickness it is around 1000m

Figures 7 and 8 show the dispersion of different fragments in case of 3D Fragmentation of four different explosive types (Comp B, RDX, TNT and Tetryl) with shell thickness values (0.2m and 0.15m). The fragment mass and initial throwing angles are randomly sampled. The maximum distance travel by fragments is around 1500m in case of0.2m shell thickness while for thickness of 0.15m shell thickness it is around 1000m

4. Probability of Damages

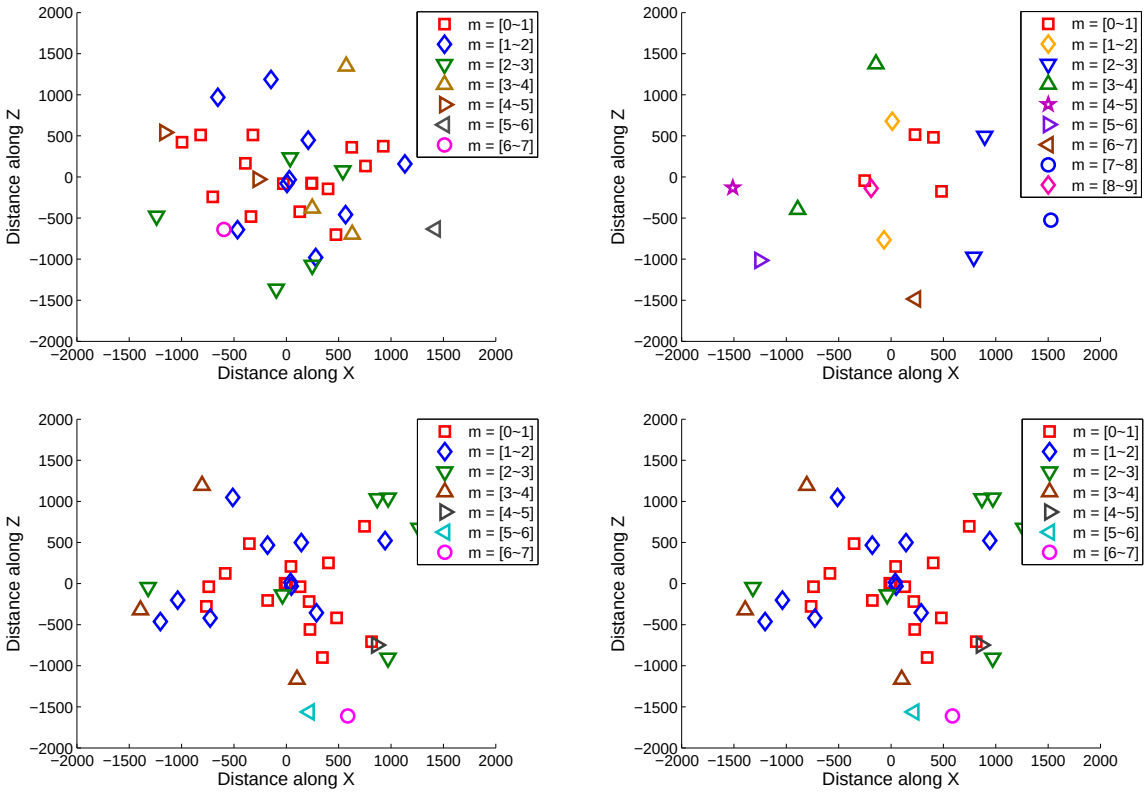

FIGURE 7. Dispersion Map with 3D Fragmentation for Shell with thickness of 0.2m

The probability that a fragment would impact a particular target (human) has been predicted using the equations.

Person in Standing Position

Figure 9 (a, b) show the probability of being hit by the minimum mass fragments in case of 2D fragmentation, when a person is in standing position, facing the explosion and taking no evasive action. It can be observed that the probability of being hit is maximum at the origin and decreases with increasing distance from the point of explosion. The probability of damage is 0.7% at the origin (fragmentation point), 0.1% at a distance of 500m and almost zero at a distance of 1000m.

Figure 10 (a, b) show the probability of being hit by the minimum mass fragments in case of 3D fragmentation. The probability of the minimum mass fragment to hit a human target is

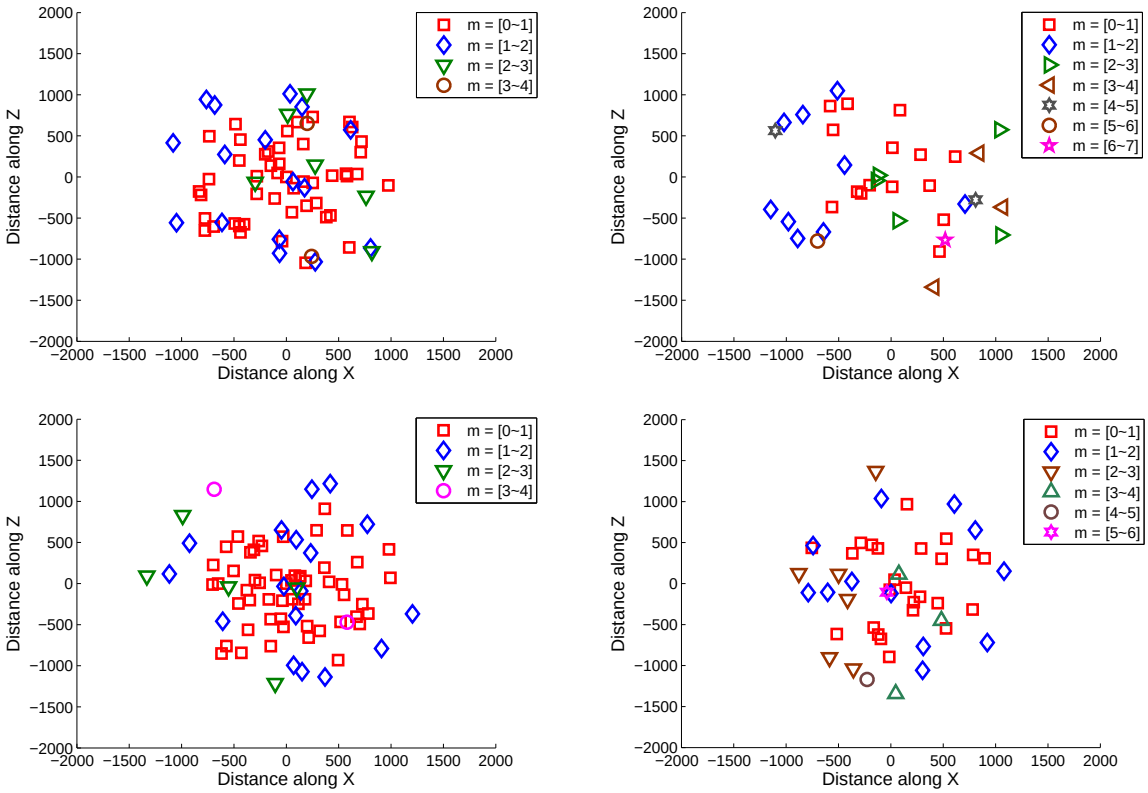

FIGURE 8. Dispersion Map with 3D Fragmentation for Shell with thickness of 0.15m

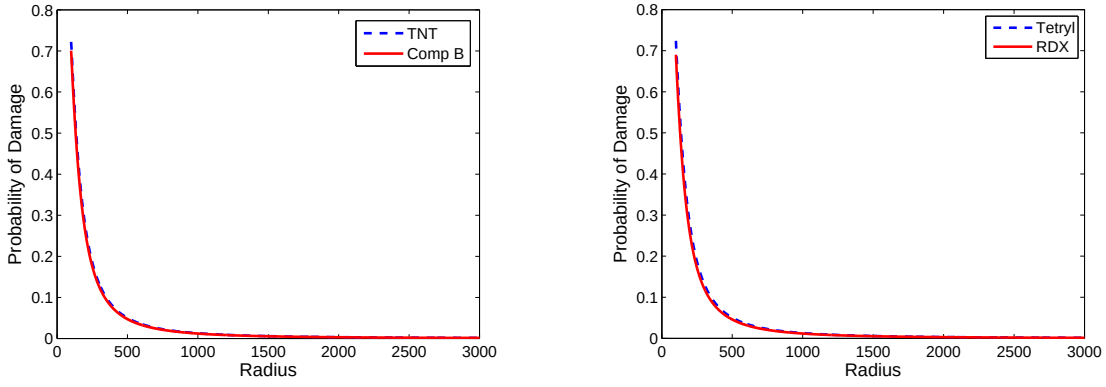

(A) (B)

FIGURE 9. Probability of Damage based on 2D Fragmentation at Standing Position

1% at the origin (fragmentation point), 0.1% at 1000m distance from the origin and negligible afterwards

Person in Assaulted Position

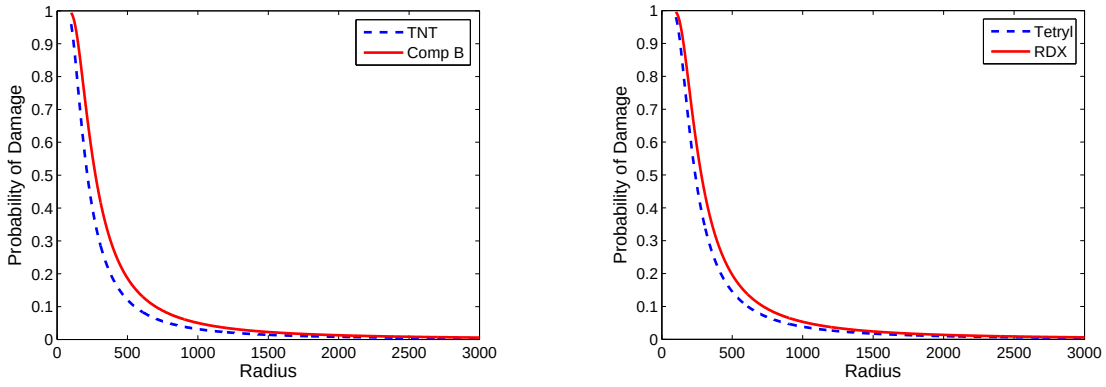

(A) (B)

FIGURE 10. Probability of Damage based on 3D Fragmentation at Standing Position

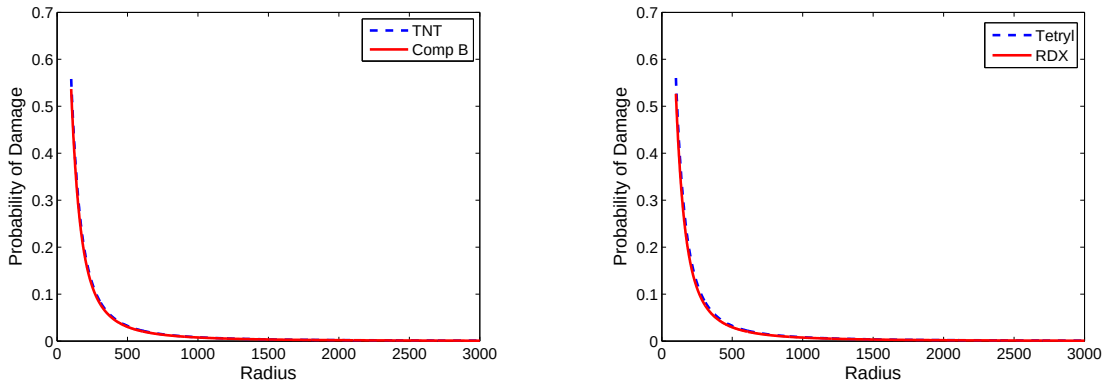

(A) (B)

FIGURE 11. Probability of Damage based on 2D Fragmentation at Assaulted Position

Figure 11(a, b) illustrate the probability of damage by the minimum mass fragments in case of 2D fragmentation, when a human is in sitting position near the point of explosion. It is evident from the graph that, for assaulted position the probability from origin (fragmentation point) is 0.6% and it starts declining until it reaches a distance 500m. At a distance of 500m probability is 0.1. After a distance of about 700m, the probability is almost zero.

Figure 12(a, b) illustrate the probability of damage by the minimum mass fragments in case of 3D fragmentation. The probability of being hit is maximum near the point of fragmentation and then starts to decline until it reaches a distance 700m. Beyond 700m range, we neglect the probability value and considered as zero.

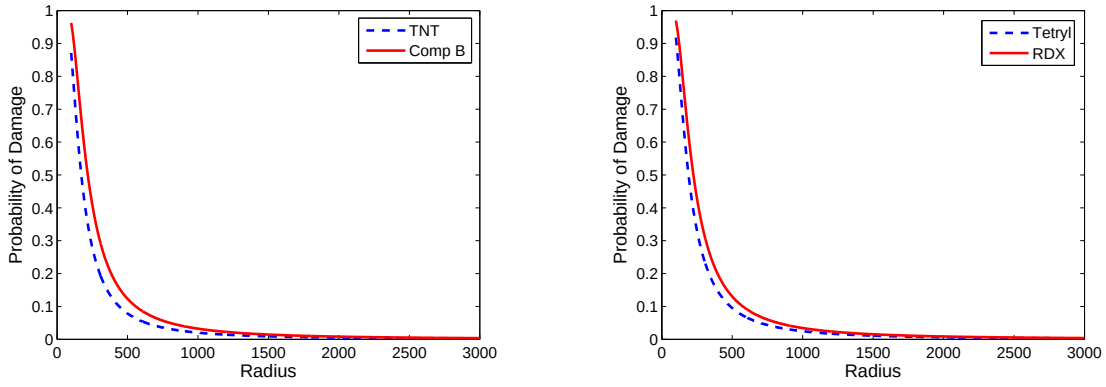

(A) (B)

FIGURE 12. Probability of Damage based on 3D Fragmentation at Assaulted Position

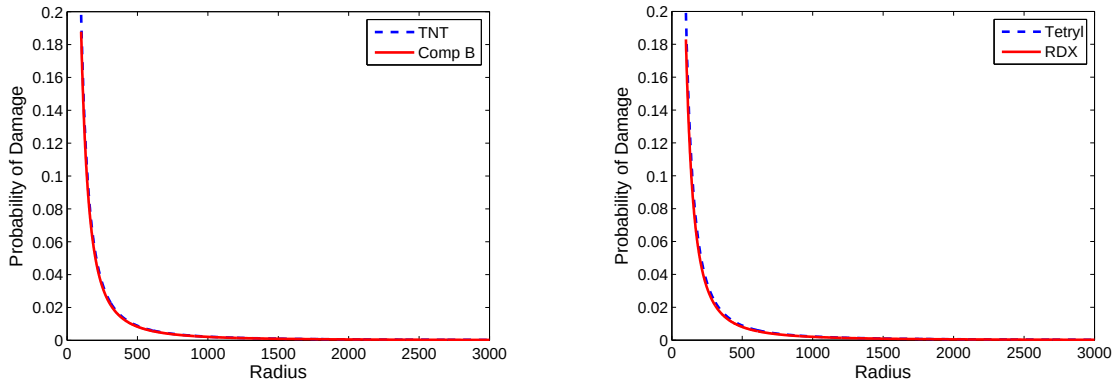

(A) (B)

FIGURE 13. Probability of Damage based on 2D Fragmentation at Supine Position

Person in Supine Position

Figure 13 (a, b) demonstrations the probability of being hit by the minimum mass fragments in case of 2D fragmentation, when a person is in supine position. For a supine position probability start with 0.2% from the fragmentation point. At a distance of 250m it reaches a value of 0.1%. After a distance of 500m the probability is almost zero.

Figure 14 (a, b) demonstrates the probability of being hit by the maximum in case of 3D fragmentation. For comp B, TNT, the probability of damage is 0.6% and 0.4% near the origin and 0.1% at 250m distance from origin. While for RDX and Tetryl probability start with

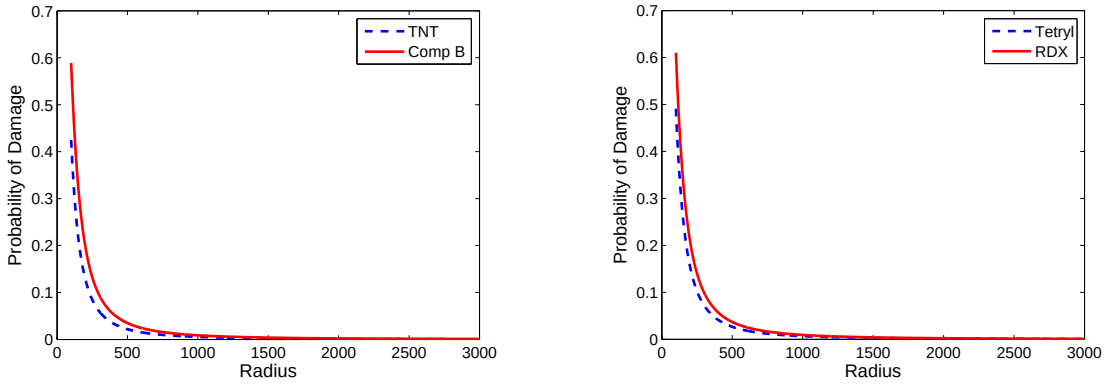

(A) (B)

FIGURE 14. Probability of Damage based on 3D Fragmentation at Supine Position

$0.6\% - 0.5\%$ values, respectively until it reaches a distance of $250m$ where the probability is around 0.1%.

5. Conclusion

The key objective of this research was to estimate the terminal impact of fragments produced in 2-D and 3-D fragmentation of cylindrical explosive munitions. Mott formulation is used for estimation of fragment mass distribution in 2D and 3D cases. Fragment trajectories under the action of constant drag and Gravity are calculated from three dimensional equations of motion. A limited parametric study is performed to estimate the risks of human injury from 2D and 3D fragmentation of cylindrical explosive munitions, by considering

- Various Explosive Types
- Different Shell Thickness

The significant conclusions of this work are summarized as follows In our analysis we estimated the limits for our mass values. For each explosive types used we considered two types of shell thickness. For each shell thickness we had different maximum mass values depending on the explosive types. Each mass value give different number of fragments counts. As we increase the mass values from minimum to maximum our fragments counts decreases sharply. The values of mass around zeros gives fragments counts which is approximately equal to the

total numbers of fragments. If the mass value is around maximum value, the possible number of fragments is around 1. If we keep increasing the mass values beyond the maximum values then our number of fragments count is less than zeros which violate the laws of nature.

In dispersion Maps minimum mass values dispersed around the fragmentation point. As we increase the mass values they dispersed away from the fragmentation point. This behavior is absorbed for each type of explosive materials. In case of shell thickness mass values varies in depth for $0.2m$ shell, while in case of $0.15m$ thickness the limit between the minimum and maximum mass value is narrow. The maximum distance travel by the fragments is around 1500 meter from the fragmentation points.

We see in dispersion Maps maximum damage area is around $1000m$ where the probability of damage is maximum. On the basis of this observation we have plotted different probability of damage for different postures of Human. In case of 2D fragmentation for standing position the probability of damage is around 0.7 while it is almost 1 in case of 3D fragmentation. In case of assaulted position it is around 0.55 in 2D fragmentation while it is almost 0.9 in case of 3D fragmentation. For supine position it is around 0.2 in case of 2D fragmentation and in case of 2D fragmentation it is 0.5.

Conflict of Interests

The authors declare that there is no conflict of interests.

REFERENCES

[1] Rosin, P., The laws governing the fineness of powdered coal. 7 (1933), 29-36.

[2] Weibull, W., A statistical theory of strength of materials, IVB-Handl. (1939).

[3] Schuhmann, E., Principles of communication, size distribution and surface calculations. 1189(1-11), 1941.

[4] Macas-Garca, A. E. M. C.-C. a. M. A. D.-D., Application of the RosinRammler and GatesGaudinSchuhmann models to the particle size distribution analysis of agglomerated cork. Materials Characterization, 52 (2) (2004), 159-164.

[5] Ouchiyama, N. S. L. R. a. J. B., A population balance approach to describing bulk attrition. Chemical Eng. Sci. 60 (5) (2005), 1429-1440.

[6] Loveland, P. J. a. W. R. W., Particle size analysis. Smith KA; Mullins CE Soil analysisphysical methods (2000), 281-314.

[7] Wu, S. Z. K. T. C. a. T. X. Y., Crushing and fragmentation of brittle sphere under double Impact test. Powder technology 143 (2004), 41-55.

[8] Mott, N. F., Fragmentation of shell casings and the theory of rupture in metals. Springer, Berlin, Heidelberg, 2006.

[9] Mott N., Linfoot E. A Theory of Fragmentation. In, Fragmentation of Rings and Shells. Shock Wave and High Pressure Phenomena. Springer, Berlin, Heidelberg, (2006).

[10] Lienau, C. C., Random Fracture for brittle solid. J. Franklin Inst. 221 (6) (1936), 769-787.

[11] Coles, P., 1991. Voronoi cosmology. Nature 349 (6307) (1991), 288.

[12] Ringler, T. L. J. a. M. G., A multiresolution method for climate system modeling, application of spherical centroidal Voronoi. Ocean Dynamics 58 (5-6) (2008), 475-498.

[13] Aurenhammer, F., Voronoi diagrams- A survey of fundamental geometric data Structure. ACM Computing Surveys (CSUR) 23(3) (1991), 345-405.

[14] Manzini, G. A. R. a. N. S., New perspectives on polygonal and polyhedral finite element methods. Mathematical Models and Methods in Applied Sciences 24 (08) (2014), 1665-1699.

[15] Kiang, T., Mass distributions of asteroids, stars and galaxies. Zeitschrift fur Astrophysik 64 (1966), 426-432.

[16] Grady, D. E. a. M. E. K., Experimental measurement of dynamic failure and fragmentation properties of metals.International journal of solids and structures 32 (17-18) (1995), 2779-2791.

[17] Grady, D. E. e. a., Comparing alternate approaches in the scaling of naturally fragmenting munitions.Switzerland. Interlaken, Proceeding of the 19th International Symposium on Ballistics, 2001.

[18] Grady, D. E., Comparison of hypervelocity fragmentation and spall experiments with TulerButcher spall and fragment size criteria. International journal of impact engineering 33.1-12 (2006), 305-315.

[19] Brown, W. K., A Theory of Sequential Fragmentation and its application in Astronomical Application.Journal of Astrophysics and Astronomy 10 (1) (1989), 89-112.

[20] Strmse, E. a. K. O. I., A modification of the Mott formula for prediction of the fragment size distribution. Propellants, Explosives, Pyrotechnics 12 (5) (1987), 175-178.

[21] Elek, P. a. S. J., Fragment Size Distribution in Dynamic Fragmentation, Geometric Probability Approach. FME Transactions 36 (2) (2008), 59-65.

[22] Elek, P. a. S. J., Size Distribution of Fragments Generated by Detonation of Fragmenting Warhead. 23rd International Symposium on Ballistics Tarragona, Spain, 2007.

[23] Szmelter, J. a. C. K. L., Prediction of Fragments Distribution and Trajectories of Exploding shells. Journal of Battlefield Technology, 10 (3) (2007), 1-7.

[24] Klein, P., Fragments and Hazards, Washington, D.C, Departments of Defense Explosives Safety Board. 1975.

[25] Zehrt Jr, W. H. a. M. M. C., Development of Primary Fragmentation Separation Distances for Cased Cylindrical Munitions, s.l., Army Engineering and Support Center Huntsville, 1998.

[26] Catovic, A. B. Z. a. J. T., Analysis of Terminal Effectiveness For Several Types of HE Projectile and Impact Angles Using Coupled Numerical CAD Technique.. s.l., 12th Seminar on New Trends in Research of Energetic Materials. 2009.

[27] TRANA, A. R. a. E., Modelling and Simulation of Ballistic Protection. MTA Review, 2015.

[28] R.W.Gurney, The Initial Velocities of Fragments from Bomb, Shell and Grenades, BRL-405, Aberdeen, Maryland, Ballistic Research Laboratory. 1943.

[29] Ngo, T. G. a. J., 2007. Blast Loading and blast effects on Structures-an Overview. Electronic Journal of Structural Engineering 7 (S1) (2007), 76-91.